GhD14 regulates plant architecture and fiber development in cotton

Liping Zhu
Shaanxi Normal University College of Life Sciences
Lingling Dou
Xianyang Normal University
Huizhi Zhang
Shaanxi Normal University College of Life Sciences
Li Zhang
Shaanxi Normal University College of Life Sciences
Cuixia Liu
Shangluo University
Jianing Yu
Shaanxi Normal University College of Life Sciences
Guanghui Xiao (guanghuix@snnu.edu.cn)
Shaanxi Normal University College of Life Sciences https://orcid.org/0000-0003-2717-8012

Research Article

Keywords: Gossypium hirsutum, Strigolactone signaling, DWARF14, plant architecture, fiber development

Posted Date: March 30th, 2021

DOI: https://doi.org/10.21203/rs.3.rs-317430/v1

Abstract

Strigolactone (SL) signaling is essential in regulating plant development. DWARF14 (D14), the SL receptor, interacts with the F-box in MORE AXILLARY GROWTH (MAX2) to modulate SL signaling. However, the biological function of D14 protein is still unknown in cotton. Here, we identified GhD14s in *Gossypium hirsutum* and resolved its function in cotton plant architecture and fiber development. The GhD14D protein was localized to both the cytoplasm and nucleus. GUS staining assay showed that GhD14D was mainly expressed in leaf primordium, inflorescence, axillary bud and stem and expression analysis revealed that *GhD14A/D* was highly expressed in stem, flower and fiber cells at 20 days post-anthesis (DPA). Silencing *GhD14A/D* gene expression in upland cotton significantly increased branch angle and reduced fiber length as well as the transcripts of secondary cell wall biosynthesis related genes. In addition, overexpression of *GhD14D* in *Atd14* mutant successfully rescued the phenotype of the *d14-1* mutant with much shoot-branching and short plant height. Our findings suggest that the *GhD14* gene contributes to shoot branch development and fiber cell development in cotton. This study deepens our understanding of the biological role of SL signaling in cotton and providing guidance for modifying cotton plant architecture and improving fiber development using genetic engineering to help us breed better cotton varieties in the future.

1 Introduction

Plant architecture refers to the organization of the plant body, includes shoot branching, branch length, branch angle, position of organs and so on in plants (Wang et al. 2008). Higher plants display various plant architectures for their different requirements. For crops, the crop yield and quality could be affected by plant architecture. After the Green Revolution, crop yields dramatically increased due to higher planting density, which was made possible by changes in plant architecture leading to shorter and more compact cultivars (Peng et al. 1999). The plant architecture is influenced by many environmental factors such as moisture and light. The drought stress reduces plant height and grain yield (Todaka et al. 2015). The dark and cold condition cause the plant to be dwarfed. Phytohormones play important roles in plant development process (Blázquez et al. 2020; Xia et al. 2019). The plant architecture also be regulated by phytohormones (Domagalska et al. 2011).

SLs, a group of sesquiterpene lactones plant hormones (Al-Babili et al. 2015; Wang et al. 2020). The SLs were known to induce germination of parasitic plants and identified as branching inhibition hormone (Kameoka et al. 2018). The biosynthesis pathway of SLs is well documented (Alder et al. 2012). The SLs biosynthesis is derived from the carotenoid pathway: first, *Dwarf 27* (*D27*) carotenoid isomerase catalyzes the conversion of all-*trans*-β-carotene into 9-*cis*-β-carotene (Alder et al. 2012). Subsequently, Carotenoid Cleavage Dioxygenase 8 (CCD8), encoded by *More Axillary Growth 4* converts 9-*cis*-β-apo-10'-carotenenal into carlactone (Alder et al. 2012). Carlactone can be further converted into 5-deoxylstrigol and other bioactive SLs via a cytochrome P450 monooxygenase, which is encoded by *More Axillary*

Growth 1 (Seto et al. 2014). Meanwhile, the biosynthesis of SLs can be regulated by zaxinone, an endogenous carotenoid-drived molecule (Wang et al. 2019; Ablazov et al. 2020). The perception for the strigolactone DWARF14 (D14), is an α/β-hydrolase (Seto et al. 2019).

The strigolactones control many aspects of plant development and abiotic stress response. The SL biosynthesis gene (HIGH TILLERING AND DWARF 1/DWARF17) increases tiller number of rice and improves rice grain yield (Wang et al. 2020). In Arabidopsis, three key repressors of the strigolactone (SL) signaling pathway (SMXL6/SMXL7/SMXL8) directly interact with two transcriptional factors and suppress their transcriptional activation of a key repressor of branching (BRC1), thus promoting branching (Xie et al. 2020). The SL could trigger polyubiquitination and degradation of SMXL2, then regulating the gene expression and hypocotyl elongation (Wang et al. 2020). The SL also control the degradation of cytokinin via activating the transcription of *CYTOKININ OXIDASE/DEHYDROGENASE 9* in rice (Duan et al. 2019).

The SL receptor, Dwarf14 (D14), is a key receptor that interacts with an F-box protein to form a Skp1-Cullin-F-BOX (SCF) complex and regulates SL signaling pathway (Nakamura et al. 2013). In soybean, the GmMAX2 interacted with the GmD14 and then forming active D14/KAI-SCF^{MAX2} complexes for function (Ahmad et al. 2020). The SCF complex then recruits SL repressor proteins to be ubiquitinated and then the SL be degraded, hence the SL repressor proteins could regulate the expression level of SL-dependent genes (Marzec. 2016). A Yoshimulactone Green (YLG) based *in vitro* assay of a high-throughput chemical screening identified a novel small molecule DL1 as a potent inhibitor of D14 that competes with endogenous SLs and increases shoot branching in Arabidopsis and rice (Yoshimura et al. 2018). In *Dendranthema* grandiflorum, *DgMAX2*, a key regulatory gene in SL signal transduction, can restore *atmax2-1* mutant branching to wild-type (WT) in Arabidopsis (Dong et al. 2013). In Populus, there are two *PtD14* genes, but only *PtD14a* was able to recover the *Atd14* mutant (Zheng et al. 2016). However the D14 in *G. hirsutum* has not been investigated.

In this study, a putative SL receptor, *GhD14*, was identified in *G. hirsutum* and it was localized to both the cytoplasm and nucleus. The expression analysis showed that *GhD14* was primarily expressed in buds, stems, flowers and 20 DPA fibers. *GhD14*-silenced plants had a phenotype of increased branch angle, reduced fiber length and the transcripts level of secondary cell wall biosynthesis related genes. Meanwhile, the *GhD14* rescued the phenotype of the *d14-1* mutant with much shoot-branching and short plant height. These result shows that *GhD14* is involved in regulating cotton architecture and fiber development, which lays a foundation for manually controlling cotton plant architecture in the future.

2 Materials And Methods

2.1 Plant materials and growth conditions

G. hirsutum cultivar Xuzhou 142 was planted in a climate-controlled greenhouse with the same condition as previously reported (Lin et al. 2019). The fibers at 0, 3, 5, 10, 15, and 20 days after anthesis (DPA),

stems, leaves, flowers from four months plants and roots form one month cotton plants were collected and frozen in liquid nitrogen immediately, then stored at -80°C until use. Seeds of wild-type *A. thaliana* (Columbia, Col-0) and *d14* mutant (Waters et al. 2012) were placed at 4°C vernalization for 48–72 hours, then surface-sterilized and germinated on 1/2 strength Murashigeand Skoog (1/2 MS) agar plates. Then, *A. thaliana* seedlings were transferred from the medium to soil pots grown in chambers at 24°C 14 h /10 h, light/dark cycle. The seeds of *Nicotiana Benthamiana* are uniformly scattered in the soil and culture conditions are the same as the *G. hirsutum*.

2.2 Bioinformatics analysis of D14 proteins

The open reading frame (ORF) of GhD14 was identified by ORF Finder (https://www.ncbi.nlm.nih.gov/orffinder/). The physicochemical properties were calculated by ExPASy online software (Gasteiger et al. 2003). The GhD14 protein secondary structure was predicted by SOPMA software with secondary structure prediction method (Geourjon et al. 1995). Three dimensional (3D) structure of GhD14D protein was constructed by SWISS-MODEL (Waterhouse et al. 2018). The DNAMAN software was used to further annotate the protein structure of GhD14s. The protein sequences of AtD14, OsD14 and GhD14s were submitted to DNAMAN software to perform multiple protein sequences alignment.

The D14 genes from two monocots (*Zea mays* and *Oryza sativa*) and 13 dicots (*Theobroma cacao, Corchorus olitorius, Cicer arietinum, Solanum pennellii, Capsicum annuum, Juglans regia, Arachis duranensis, Glycine max, Abrus precatorius, Phtheirospermum japonicum, Striga hermonthica, Orobanche cernua and Arabidopsis thaliana*) were selected for phylogenetic analysis. The full-length protein sequences of these homologous were obtained from the National Center for Biotechnology Information (NCBI). Phylogenetic tree was constructed by MEGA 7.0 with the Neighboring-Joining (NJ) method and 1000 bootstrap replications (Kumar et al. 2016).

2.3 DNA, RNA extraction and expression analysis of *Ghd14*

DNA extracted from cotton leaves using CTAB method (Huang et al. 2000). The total RNA of fibers at 0, 3, 5, 10, 15 and 20 days post-anthesis (DPA) and cotton roots, stems, leaves, and flowers were extracted by the PureLinkTM RNA mini kit (Invitrogen, Lot no.1687455, USA) according to the manual instructions. First-strand complementary DNA (cDNA) was reverse-transcribed from 2 μg of the total RNA by the description of PrimeScriptTM RT reagent Kit with gDNA Eraser (TaKaRa, Code No. RR047A, Japan).

The primers were designed by OLIGO 7.0 (Rychlik. 2007). For expression analysis, the ubiquitin gene *GhUBQ7* was used as a housekeeping gene (Xiao et al. 2016). All primers in this work are listed in Supplementary Table S1. The qRT-PCR experiments were performed using SYBR® Premix Ex Taq™ II (Takara, Japan) kit on a Bio-Rad Real Time PCR detection system (Bio-Rad CFX96Touch, USA) with the following reaction parameters: 94°C for 2 min, followed by 40 cycles of 94°C for 30 s and 60°C for 30 s. The $2^{-\Delta\Delta CT}$ method was used to calculate the relative expression levels of the target genes. All data were statistically analyzed using by One-way ANOVA method by SigmaStat software with default parameters (Ji et al. 2003).

2.4 Cloning, plasmid construction and transformation

The protein sequence of AtD14 was downloaded from TAIR database, and used as a query sequence to against the *G. hirsutum* protein genome database (ZJU_v2.1). The most similarity genes to AtD14 in *G.hirsutum* were recognized as GhD14s. The gene was amplified from *G. hirsutum* cDNA with PrimeSTAR® Max DNA Polymerase (TaKaRa, Japan) and sequenced by TSINGKE company (Beijing, China).

The 1715 bp upstream genomic DNA sequence of the initiation codon (ATG) from *GhD14D* was cloned as the promoter sequence from Xuzhou 142 DNA and full-length CDS of *GhD14* were amplified from Xuzhou 142 cDNA. For overexpression of *GhD14D* experiment, the full-length of *GhD14D* CDS sequence was assembled into pCAMBIA1305 by In-Fusion® HD Cloning Kit (Vazyme Biotech, China) according to the instructions. For β-glucuronidase (GUS) staining analysis, the *GhD14D* promoter sequences was introduced into pCAMBIA2300 to drive the GUS gene expression. All the final constructs were transformed into *A. thaliana* and *N. benthamiana* by *Agrobacterium tumefaciens* mediated transformation method as previously described (Cheng et al. 2018). In addition, the full-length CDS of *GhD14D* was cloned into pTF486-GFP and pCHF3-GFP to generate the 35S::GhD14-GFP construct for subcellular localization assays. Two primers in pCAMBIA1305 were used for identification of whether *A. thaliana* contain pCAMBIA1305: *GhD14D*. All the primers used in vector construction are listed in Supplementary Table S1. Meanwhile, one month old *A. thaliana* seedlings was used for observation of the rosette leaves of seedlings and leaves phenotype and Two and a half month *A. thaliana* was used for the whole plants phenotype observation.

2.5 GUS staining analysis

For GUS staining analysis, the GhD14Dpro::GUS construct was introduced into *A. tumefaciens* strain GV3101 and subsequently transformed into *A. thaliana* using the floral dip method (Lloyd et al. 1986). Transgenic plants were selected on solid half-strength MS media plates containing 50 μg/mL chloramphenicol. The selected transgenic seedlings were further validated by genomic PCR. Various tissue at different developmental stages were collected, and stained with GUS staining solution according to the instructions. The microscop (Nikon, Japan) was used to observe the GUS staining result.

2.6 Transient expression of GhD14D-GFP

For subcellular localization of GhD14D, the fused GhD14D-GFP vectors were transiently expressed in *A. thalinan* protoplast and *N. benthamiana* according to previous studies (Abel et al. 1994; Cheng et al. 2018). The two fusion constructs pTF486-GFP and pCHF3-GFP were used for transient expression GhD14D-GFP in *A. thaliana* protoplast and in *N. benthamiana* epidermis cells, respectively. In addition, the nuclei staining, the chemical reagent 4', 6'-diamidino-2-phenylindole (DAPI) staining method was used to confirm the nuclei localization of GhD14D (Liang et al. 2018). The positive transgenic plants were used for *in vivo* subcellular localization analysis using a confocal microscope (Nikon, Japan).

2.7 Virus-induced *GhD14A/D* gene silence in *G. hirsutum*

The binary CLCr vectors pCLCrVA and pCLCrVB were used for virus-induced gene silence (VIGS) analysis (Gu et al. 2014). Three fragments of *GhD14A/D* gene were amplified using cDNA with the primers listed in Supplementary Table S1. The PCR fragments were inserted into pCLCrVA and these vectors were transformed into *A. tumefaciens* GV3101 by electroporation. The *A. tumefaciens* culture containing pCLCrVA or the constructed vectors were mixed with an equal volume of an *A. tumefaciens* culture containing pCLCrVB to generate the mixed *A. tumefaciens* solutions for infiltration. The mixed solutions were infiltrated into fully expanded cotyledons of 10-day-old cotton seedlings with 15 plants through vacuum infiltration (Gao et al. 2011). The inoculated seedlings were then transferred to a dark climate-controlled greenhouse at 25°C. The one month old seedling leaves and 25 DPA fibers from negative control and *GhD14A/D*-VIGS cotton plants were chosen to assess the silence effects of *GhD14A/D* gene by qRT-PCR experiment. The sixth branches from bottom to top were used for detecting the angle of the monopodial branch

3 Results

3.1 Identification of the GhD14 in *G. hirsutum*

The AtD14 protein sequence was used as the query sequence to against the *G. hirsutum* genome (Hu et al. 2019) to obtain the D14 protein in *G. hirsutum*. The sequences GH_A02G1790.1 and GH_D03G0270.1 in the cotton genome were the most similar to AtD14 and were chosen as the candidate orthologs of AtD14 and named GhD14A and GhD14D, respectively. The GhD14A and GhD14D have one intron, contain 816 base pairs (bp) (Supplementary Fig. 1A), 271 amino acids (Fig. 1A) and have a molecular weight of 19.9 kDa and 30.0 kDa, respectively.

3.2 Conserved domain and promoter analysis of GhD14s

The AtD14 protein structure in *A. thaliana* has been reported as an α/β hydrolase (Li et al. 2020). We compared the protein sequences of GhD14A, GhD14D and AtD14, and identified eight α-helixes, five η-helixes and seven β-strands in D14 protein (Fig. 1B, Supplementary Fig. 1B, C). There are three catalytic residues, S95, D217 and H246 in GhD14A and GhD14D protein sequences (Fig. 1B). The sequence similarities of AtD14 with GhD14A and GhD14D were 52.7% and 53.5%, respectively. As *GhD14A* and *GhD14D* have 97.4% similarity in coding sequences, we cloned *GhD14D* from *G. hirsutum* cultivar Xuzhou 142 and used it as the representative *GhD14* gene for *cis*-elements distribution, subcellular location, GUS and overexpression analysis.

The *cis*-element distribution of 1,715 bp *GhD14D* promoter sequence and promoter driven GUS expression were investigated to study the potential function of *GhD14D*. The *GhD14D* promoter has high A and T content, and typical *cis*-elements TATA-box and CAAT-box (Supplementary Figure S2), which are consistent with the characteristics of other plant promoters (Zhang et al. 2016). The auxin responsiveness *cis*-element AUXRR-core and jasmonic acid methyl ester (MeJA) responsiveness regulatory element CGTCA-motif were also present in the *GhD14D* promoter region (Supplementary Figure

S2), indicating that auxin and MeJA might function in regulating *GhD14D* gene expression via combine the corresponding *cis*-elements present in the promoter of *GhD14D*.

3.3 Phylogenetic analysis of GhD14s

To explore the evolutionary relationships among GhD14D and other fifteen D14s from typical higher plant species, we performed phylogenetic analysis of D14 proteins from *G. hirsutum* and other fifteen higher plant species using MEGA 7.0 software with Neighboring-Joining (NJ) method and 1000 bootstrap replications. The phylogenetic tree showed that the D14s in sixteen higher plants have the same evolutionary origin. The D14s was resolved into two evolutionary branches in phylogenetic tree and both of which contain D14 proteins from monocotyledons and dicotyledons. Meanwhile, GhD14s was more closely related to eudicots, and was most closely related to *T. cacao*, with moderate bootstrap support of 79% (Supplementary Figure S3).

3.4 GhD14D is localized to the cytoplasm and nucleus

The pTF486-GhD14D:GFP vector was constructed to investigate the subcellular location of GhD14D protein and DAPI staining was used to test whether the GhD14D protein was localized in the nucleus. The pTF486-GhD14D:GFP was transiently expressed in *A. thaliana* protoplasts and the cells were stained with DAPI, and then examined using confocal microscopy. The results showed that GhD14D-GFP fusion protein was accumulated throughout the nucleus and cytoplasm and was also co-localized with DAPI (Fig. 2A). The pCHF3-GhD14D:GFP was bombarded into tobacco epidermal cells by agroinfiltration to further confirm the subcellular localization of GhD14D protein. We found the green fluorescence of GhD14D-GFP distributed in the cytoplasm and nucleus and the fluorescence of GhD14D-GFP coincided with the DAPI fluorescence, confirming that GhD14D protein is co-localized in the cytoplasm and nucleus (Fig. 2B). Both GhD14D-GFP fusion protein and DAPI methods in *A. thaliana* protoplast and tobacco epidermal cells clearly showed strong nucleus and cytoplasm localization, indicating that the hydrolase GhD14D functions in the cytoplasm and nucleus.

3.5 Expression patterns of *GhD14A/D*

Expression patterns of *GhD14A/D* in fibers at 0, 3, 5, 10, 15 and 20 days post-anthesis (DPA) and root, stem, leaf, and flower were investigated to explore the function of *GhD14* using quantitative real-time PCR (qRT-PCR). Since *GhD14A* and *GhD14D* have 97.43% coding sequence similarity and they can't separate with specific primer, the expression level of *GhD14A/D* was investigated. As shown in Fig. 2, *GhD14A/D* gene transcripts were increased during the fiber development with peak value at 20 DPA (Fig. 3A), and abundantly expressed in flower and stem (Fig. 3B), indicating that *GhD14A/D* may function in fiber, flower and stem development.

In order to test the tissue specific expression of *GhD14D*, the *GhD14D* promoter driving *GUS* gene expression in *A. thaliana* was visualized by histochemical staining of transgenic *A. thaliana*. The color of transgenic *A. thaliana* seedlings represents the promoter driven GUS gene expression. As shown in Fig. 4,

the *GhD14D* promoter-driven *GUS* gene was highly expressed in buds, stems and flowers (Fig. 4). These observations demonstrated that *GhD14D* may play important role in buds, stems and flowers.

3.6 *GhD14A/D* gene silencing in cotton increased branch angles and reduced fiber length

Virus-induced gene silencing (VIGS) is an efficient and rapid method to reduce gene transcripts and investigate gene functions in plants (Gu et al. 2014). To further uncover potential functions of *GhD14* in cotton, the VIGS strategy was used to reduce *GhD14A/D* transcript levels in *G. hirsutum*. Positive control of *GhPDS* gene silence shows in Supplementary Figure S5. Expression levels of the *GhD14A/D* gene were detected using qRT-PCR strategy and the result showed that *GhD14A/D* gene expression was significantly reduced in *GhD14A/D*-silenced plants compared with that in the control plants (CLCrVA) (Fig. 5A). The phenotype of branch angles of control and VIGS plants (*GhD14A/D*-V1, *GhD14A/D*-V2 and *GhD14A/D*-V3) showed that the monopodial branch angles were significantly increased in *GhD14A/D*-silenced plants compared with the negative control plants (CK). The branch angles of *GhD14A/D*-silenced plants were increased about two times compared with the CK (Fig. 5B, C, Supplementary Figure S4). In order to explore the potential functions of *GhD14A/D* in cotton fiber development. The fiber length was observed after *GhD14A/D* silencing, and the result showed that the cotton fiber length was significantly reduced in *GhD14A/D*-silenced plants (Fig. 5D, E), indicating the *GhD14A/D* gene may play a critical role in cotton fiber elongation. In general, reducing *GhD14A/D* gene expression led to wider branch angles and decreased fiber length, suggesting that *GhD14A/D* functions in cotton architecture and fiber development.

3.7 *GhD14A/D* gene silencing in cotton reduce the transcripts of secondary cell wall biosynthesis genes

The cotton fiber is produced by the specific elongation of cell in ovule epidermal and cell wall biosynthesis is required during the fiber elongation process. To further investigate the mechanism of *GhD14A/D* in regulating fiber development, the relative expression level of secondary cell wall biosynthesis genes (Sun et al. 2017) was investigated in *GhD14A/D*-silenced plants. As shown in Fig. 6, The six genes (*GhLBD30*, *GhCesA7*, *GhMYB46*, *GhXCP1*, *GhIRX8* and *GhXCP2*) related secondary cell wall biosynthesis were down regulated in *GhD14A/D*-silenced plant, while other three genes (*GhIRX10*, *GhCesA8* and *GhCesA4*) related secondary cell wall biosynthesis have no significant difference in expression levels compare with the negative control (CLCrVA) (Fig. 6). This result demonstrates that downregulating of *GhD14* gene expression reduced the transcripts of genes involved in secondary cell wall biosynthesis.

3.8 Overexpression of *Ghd14d* rescued the *d14* mutant phenotype in Arabidopsis

Overexpression of *GhD14D* in the *d14* Arabidopsis mutant, a heterologous complementation approach, was performed to further explore the function of *GhD14D* in stem development and shoot branching, since *AtD14* is the receptor of SLs and has essential functions in the SL signal transduction process (Chevalier et al. 2014). The pCAMBIA1305-35S-*GhD14D* was constructed and transformed into *A. thaliana* mutant *d14-1*. The seven transgenic lines were obtained after PCR detection (Supplementary Figure S6). The third generation of six transgenic lines with stable and highly expressed *GhD14A/D* was used for further analysis. As shown in Fig. 6, mutant *d14-1* plants had smaller length-width ratio of leaf (Fig. 7A, B) and more shoot branches as well as shorter plant height (Fig. 6C, D, E) compared with wild-type *A. thaliana* plants. Overexpression of *GhD14D* in *A. thaliana d14-1* mutant restored the leaf phenotypes and the number and length of branches to the phenotype of wild-type plants (Fig. 7). The phenotype of the *d14-1* mutant with more shoot branches and short stature could be rescued by *GhD14D* and there was no significant phenotype difference between wild-type *A. thaliana* lines and *d14-1*/35S:*GhD14D* transgenic lines (Fig. 7). These results suggested that *GhD14D* and *AtD14* may have similar functions in regulating branching number, plant height, petiole length, and length-width ratio of leaf.

4 Discussion

In China, modern agricultural cultivation of cotton requires moderately short and compact varieties to adapt to mechanical operations (Su et al. 2018). The short and compact characteristics are mainly controlled by plant architecture, which is regulated by plant hormones, such as auxins and strigolactones (SLs) (Beveridge et al. 2003; McSteen et al. 2005; Ongaro et al. 2008; Domagalska et al. 2011). SLs have been recognized as a new class of hormones that participate in regulating plant architectures in terms of shoot branching, lateral roots, shoot gravitropism and stem secondary thickening (Wang et al. 2020). Branching is a highly plastic determinant of plant shape to allow plants to respond to environmental stresses (Evers et al. 2011). Shoot branching is a ubiquitous phenomenon in higher plants and a basic characteristic of plant growth, that is essential in determining plant architecture.

Cotton is an important source of protein and oil and cotton fiber is commonly used as natural fiber in the textile industry, hence, regulating growth and controlling branching are essential for cotton cultivation. Several key genes involved in the SL biosynthesis signaling pathway and participating in plant architecture development, especially shoot-branching have been identified (Beveridge et al. 2010). In this study, a homolog of AtD14 was cloned from upland cotton cultivar Xuzhou 142 and named GhD14s. GhD14s showed high identity with AtD14 (53.5%). The D14 functional domains were conserved in cotton and the model plants rice (monocotyledon) and Arabidopsis (dicotyledon) (Fig. 1). Phylogenetic analysis showed that the D14s in higher plants have a close relationship with D14s from other higher plants (Supplementary Figure S3). The conservation of D14 among different species indicates it play critical role in higher plants.

Subcellular localization results showed that GhD14D is localized to the nucleus and cytoplasm, which is consistent with the localization results of the D14 genes in Arabidopsis and rice (Chevalier et al. 2014;

Yao et al. 2018). The subcellular localization results provided evidence that GhD14D functions in both the nucleus and cytoplasm. GUS staining showed that D14 in rice was mainly expressed in parenchyma cells surrounding the xylem in leaves, stems and axillary buds (Arite et al. 2009). In this study, the GhD14D pro::GUS gene expression was mainly observed in the buds, stems and flowers (Fig. 4). The transcripts of *GhD14D* in cotton were also significantly accumulated in stem, leaf, flower and 20 DPA fibers (Fig. 3). These results demonstrate that *GhD14D* functions in stem, leaf, flower and fiber development. Previous studies in other plants found that *D14* was involved in the development of stem, leaf and flower: The *d14* mutant had a larger stomatal aperture in leaf, slower abscisic acid (ABA)-mediated stomatal closure, lower anthocyanin and reduced plant senescence under drought stress (Li et al. 2020). OsMADS57 interacts with TEOSINTE BRANCHED1 (OsTB1) and targets OsD14 to control the outgrowth of axillary buds in rice (Guo et al. 2013).

The OsD14 is the receptor of SL protein, which acts as a new component of the SL-dependent branching inhibition pathway and inhibits rice tillering (Arite et al. 2009). AtD14 hydrolyzes SLs into a D-ring-derived intermediate CLIM and irreversibly binds CLIM to trigger SL signal transduction, thus regulating shoot branching in Arabidopsis (Yao et al. 2016). Furthermore, overexpression of *GhD14D* in the *d14* mutant, was performed to further explore the function of *GhD14D* in stem development and shoot branching. As a result, overexpression of *GhD14D* in *AtD14* mutant (*d14-1*) reduced the mean number of branches and restored the plant height (Fig. 7). Meanwhile, the branching and leaf phenotypes were restored to wild-type plants phenotype and there was no significant difference between wild-type plants and *d14-1/35S::GhD14D* transgenic lines. The phenotype of the *d14-1* mutant with fewer shoot branches and higher stature could be rescued via *GhD14D* overexpression in *d14* mutant, suggesting that *GhD14D* and *AtD14* may have similar functions in regulating branching number, plant height, petiole length, and length-width ratio of leaf. Consistently, the *OsD14* gene also restored the phenotype of d14 to the wild type both in plant height and tiller development in rice (Yao et al. 2018).

The *GhD14A/D* had high expression levels in flower, stem, leaf, and 20 DPA fibers, but was weakly expressed in cotton root (Fig. 3). In rice, transcripts of *D14* were highly accumulated in leaves and the first leaf buds, but not in root tip (Arite et al. 2009). In petunia, high expression levels of *DAD2* were observed in axillary bud and leaf, but not in root (Hamiaux et al. 2012). In chrysanthemum, *DgD14* had the highest expression level in stem, followed by node, and was only weakly expressed in root (Wen et al. 2015). These results reflect that the *D14* gene may not be involved in root structural development. The *GhD14A/D* showed high expression level at 20 DPA fibers (Fig. 3), and this stage is the secondary cell wall thickening stage (Zhang et al. 2015). Meanwhile, silencing the *GhD14A/D* gene expression reduced the fiber length (Fig. 5) and the expression levels of the secondary cell wall biosynthesis related genes (Fig. 6). These results indicating that *GhD14* might play a role in fiber development through impact secondary cell wall biosynthesis of cotton fiber. In the future, molecular mechanisms and regulatory relationships between *GhD14* and secondary cell wall biosynthesis needs to be further investigated to deep our understanding of the strigolactone and secondary cell wall biosynthesis.

The *GhD14A/D* gene silencing enhanced fruit branch angles and reduced fiber length in cotton (Fig. 5), indicating that the *GhD14A/D* transcripts accumulation level affects cotton plant architecture and fiber length. The plant architecture is also regulated by auxin, cytokinin, and gibberellic acid (GA). D14 is the receptor of SL, which involved in plant stature and inhibition of plant shoot branching (Arite et al. 2009). The strigolactone signal can regulate the auxin polar transport and the cytokinin content in the stem (Ferguson et al. 2009). In the future, molecular mechanisms and regulatory relationships between *GhD14* and auxin or cytokinin should be examined to deepen our understanding of strigolactone signaling in cotton architecture. Although we did not investigate this, we speculate that *GhD14* might regulate branch number and angles through auxin and GA in cotton. In the future, molecular mechanisms and regulatory relationships between *GhD14* and auxin or GA should be examined to deepen our understanding of SL signaling in cotton architecture.

5 Conclusion

Strigolactone (SL) signaling functions directly in regulating plant development. DWARF14 (D14), a non-canonical SL receptor, interacts with the F-box protein MAX2 to modulate SL signaling in rice and *Arabidopsis*. In this study, the *GhD14D* was cloned from *G. hirsutum*, which containing a hydrolase fold motif, and had similar protein domains as typical D14 proteins. Subcellular localization analysis revealed that GhD14D was located in the cytoplasm and nucleus. qRT-PCR results showed that *GhD14A/D* was highly expressed in stem, flower and 20 DPA fiber cells; GUS staining assay indicated that *GhD14D* was mainly expressed in leaf primordium, inflorescence, axillary bud and stem. Reducing the transcripts of *GhD14A/D* in cotton significantly increased branch angle and reduced fiber length and the transcripts of secondary cell wall biosynthesis related genes. In addition, overexpression of *GhD14D* successfully rescued the phenotype of *Arabidopsis d14* mutant with reduced shoot-branching, length-width ratio of rosette leaves and plant height. These results indicate that *GhD14D* contributes to fiber development and plant architecture development in cotton, which will lay a foundation for manipulating cotton plant architecture by genetic engineering and provide a candidate gene for producing cultivars with ideal architectures in the future.

Declarations

Author contributions statement LZ. and LP-Z. performed the experiments; LZ. and CL. analyzed the data; LD. and HZ. performed software application and data visualization; LP-Z. and GX. wrote the paper; JY. and GX. conceived and designed the experiments. All authors read and approved the final manuscript.

Funding This work is supported by the Natural Science Basic Research Plan in the Shaanxi Province of China (2019JQ-062 and 2020JQ-410), Shaanxi Youth Entrusted Talent Program (20190205), Shaanxi Postdoctoral Project (2018BSHYDZZ76), Fundamental Research Funds for Central Universities (GK201903064, GK202002005 and GK202001004), Young Elite Scientists Sponsorship Program by CAST (2019-2021QNRC001) and State Key Laboratory of Cotton Biology Open Fund (CB2020A12).

Declarations

Conflicts of interest The authors have no conflict of interest to declare.

Consent for publication All authors have read and approved the final manuscript.

References

1. Abel S, Theologis A (1994) Transient transformation of Arabidopsis leaf protoplasts: a versatile experimental system to study gene expression. Plant J 5:421–427. https://doi.org/10.1111/j.1365-313x.1994.00421.x
2. Ablazov A, Mi J, Jamil M et al (2020) The apocarotenoid zaxinone is a positive regulator of strigolactone and abscisic acid biosynthesis in Arabidopsis roots. Front Plant Sci 11: https://doi.org/10.3389/fpls.2020.00578
3. Ahmad MZ, Rehman NU, Yu S et al (2020) GmMAX2-D14 and -KAI interaction-mediated SL and KAR signaling play essential roles in soybean root nodulation. Plant J 101:334–351. https://doi.org/10.1111/tpj.14545
4. Al-Babili S, Bouwmeester HJ (2015) Strigolactones, a novel carotenoid-derived plant hormone. Annu Rev Plant Biol 66:161–186. https://doi.org/10.1146/annurev-arplant-043014-114759
5. Alder A, Jamil M, Marzorati M et al (2012) The path from beta-carotene to carlactone, a strigolactone-like plant hormone. Science 335: 1348– https://doi.org/10.1126/science.1218094
6. Arite T, Umehara M, Ishikawa S, et al (2009) d14, a strigolactone-insensitive mutant of rice, shows an accelerated outgrowth of tillers. Plant Cell Physiol 50:1416– https://doi.org/10.1093/pcp/pcp091
7. Beveridge CA, Kyozuka J (2010) New genes in the strigolactone-related shoot branching pathway. Curr Opin Plant Biol 13:34– https://doi.org/10.1016/j.pbi.2009.10.003
8. Beveridge CA, Weller JL, Singer SR et al (2003) Axillary meristem development. Budding relationships between networks controlling flowering, branching, and photoperiod responsiveness. Plant Physiol 131:927– https://doi.org/10.1104/pp.102.017525
9. Blázquez MA, Nelson DC, Weijers D (2020) Evolution of plant hormone response pathways. Annu Rev Plant Biol 71:327-353. https://doi.org/10.1146/annurev-arplant-050718-100309
10. Cheng C, Li C, Wang D et al (2018) The soybean GmNARK affects ABA and salt responses in transgenic *Arabidopsis thaliana*. Front Plant Sci 9:514. https://doi.org/10.3389/fpls.2018.00514
11. Chevalier F, Nieminen K, Sanchez-Ferrero JC et al (2014) Strigolactone promotes degradation of DWARF14, an alpha/beta hydrolase essential for strigolactone signaling in Arabidopsis. Plant Cell 26:1134– https://doi.org/10.1105/tpc.114.122903
12. Domagalska MA, Leyser O (2011) Signal integration in the control of shoot branching. Nat Rev Mol Cell Biol 12:211– https://doi.org/10.1038/nrm3088
13. Dong L, Ishak A, Yu J et al (2013) Identification and functional analysis of three MAX2 orthologs in chrysanthemum. J Integr Plant Biol 55:434– https://doi.org/10.1111/jipb.12028

14. Duan J, Yu H, Yuan K, et al (2019) Strigolactone promotes cytokinin degradation through transcriptional activation of CYTOKININ OXIDASE/DEHYDROGENASE 9 in rice. Proc Natl Acad Sci U S A 116:14319-14324. https://doi.org/10.1073/pnas.1810980116
15. Evers JB, van der Krol AR, Vos J et al (2011) Understanding shoot branching by modelling form and function. Trends Plant Sci 16:464– https://doi.org/10.1016/j.tplants.2011.05.004
16. Ferguson BJ, Beveridge CA (2009) Roles for auxin, cytokinin, and strigolactone in regulating shoot branching. Plant Physiol 149:1929– https://doi.org/10.1104/pp.109.135475
17. Gao X, Wheeler T, Li Z et al (2011) Silencing *GhNDR1* and *GhMKK2* compromises cotton resistance to Verticillium wilt. Plant J 66:293– https://doi.org/10.1111/j.1365-313X.2011.04491.x
18. Gasteiger E, Gattiker A, Hoogland C et al (2003) ExPASy: The proteomics server for in-depth protein knowledge and analysis. Nucleic Acids Res 31:3784– https://doi.org/10.1093/nar/gkg563
19. Geourjon C, Deleage G (1995) SOPMA: significant improvements in protein secondary structure prediction by consensus prediction from multiple alignments. Comput Appl Biosci 11:681– https://doi.org/10.1093/bioinformatics/11.6.681
20. Gu Z, Huang C, Li F et al (2014) A versatile system for functional analysis of genes and microRNAs in cotton. Plant Biotechnol J 12:638–649. https://doi.org/10.1111/pbi.12169
21. Guo S, Xu Y, Liu H et al (2013) The interaction between OsMADS57 and OsTB1 modulates rice tillering via DWARF14. Nat Commun 4:1566. https://doi.org/10.1038/ncomms2542
22. Hamiaux C, Drummond RS, Janssen BJ, et al (2012) DAD2 is an alpha/beta hydrolase likely to be involved in the perception of the plant branching hormone, strigolactone. Curr Biol 22:2032– https://doi.org/10.1016/j.cub.2012.08.007
23. Hu Y, Chen J, Fang L et al (2019) *Gossypium barbadense* and *Gossypium hirsutum* genomes provide insights into the origin and evolution of allotetraploid cotton. Nat Genet 51:739– https://doi.org/10.1038/s41588-019-0371-5
24. Huang J, Ge X, Sun M (2000) Modified CTAB protocol using a silica matrix for isolation of plant genomic DNA. Biotechniques 28:432– https://doi.org/10.2144/00283bm08
25. Ji SJ, Lu YC, Feng JX et al (2003) Isolation and analyses of genes preferentially expressed during early cotton fiber development by subtractive PCR and cDNA array. Nucleic Acids Res 31:2534– https://doi.org/10.1093/nar/gkg358
26. Kameoka H, Kyozuka J (2018) Spatial regulation of strigolactone function. J Exp Bot. 69:2255-2264. https://doi.org/10.1093/jxb/erx434
27. Kumar S, Stecher G, Tamura K (2016) MEGA7: Molecular evolutionary genetics analysis version 7.0 for bigger datasets. Mol Biol Evol 33:1870– https://doi.org/10.1093/molbev/msw054
28. Li W, Nguyen KH, Chu HD et al (2020) Comparative functional analyses of DWARF14 and KARRIKIN INSENSITIVE 2 in drought adaptation of *Arabidopsis thaliana*. Plant J 103:111– https://doi.org/10.1111/tpj.14712

29. Liang J, De Castro A, Flores L (2018) Detecting protein subcellular localization by green fluorescence protein tagging and 4',6-diamidino-2-phenylindole staining in caenorhabditis elegans. J Vis Exp 137. https://doi.org/10.3791/57914
30. Lin J, Cai Y, Huang G, et al (2019) Analysis of the chromatin binding affinity of retrotransposases reveals novel roles in diploid and tetraploid cotton. J Integr Plant Biol. 61:32-44. https://doi.org/10.1111/jipb.12740
31. Lloyd AM, Barnason AR, Rogers SG et al (1986) Transformation of *Arabidopsis thaliana* with *Agrobacterium tumefaciens*. Science 234:464– https://doi.org/10.1126/science.234.4775.464
32. Marzec M (2016) Perception and signaling of strigolactones. Front Plant Sci 7:1260. https://doi.org/10.3389/fpls.2016.01260
33. McSteen P, Leyser O (2005) Shoot branching. Annu Rev Plant Biol 56:353– https://doi.org/10.1016/j.pbi.2003.10.002
34. Nakamura H, Xue YL, Miyakawa T, et al (2013) Molecular mechanism of strigolactone perception by DWARF14. Nat Commun 4:2613. https://doi.org/10.1038/ncomms3613
35. Ongaro V, Bainbridge K, Williamson L et al (2008) Interactions between axillary branches of Arabidopsis. Mol Plant 1:388– https://doi.org/10.1093/mp/ssn007
36. Peng J, Richards DE, Hartley NM et al (1999) 'Green revolution' genes encode mutant gibberellin response modulators. Nature 400:256–261. https://doi.org/10.1038/22307
37. Rychlik W (2007) OLIGO 7 primer analysis software. Methods Mol Biol 402:35– https://doi.org/10.1007/978-1-59745-528-2_2
38. Seto Y, Sado A, Asami K et al (2014) Carlactone is an endogenous biosynthetic precursor for strigolactones. Proc Natl Acad Sci USA 111:1640–1645. https://doi.org/10.1073/pnas.1314805111
39. Seto Y, Yasui R, Kameoka H et al 2019 Strigolactone perception and deactivation by a hydrolase receptor DWARF14. Nat Commun 101: https://doi.org/10.1038/s41467-018-08124-7
40. Su J, Li L, Zhang C et al (2018) Genome-wide association study identified genetic variations and candidate genes for plant architecture component traits in Chinese upland cotton. Theor Appl Genet 131:1299– https://doi.org/10.1007/s00122-018-3079-5
41. Sun X, Wang C, Xiang N et al (2017) Activation of secondary cell wall biosynthesis by miR319-targeted TCP4 transcription factor. Plant Biotechnol J 15:1284–1294. https://doi.org/10.1111/pbi.12715
42. Todaka D, Shinozaki K, Yamaguchi-Shinozaki K (2015) Recent advances in the dissection of drought-stress regulatory networks and strategies for development of drought-tolerant transgenic rice plants. Front Plant Sci 6:84. https://doi.org/10.3389/fpls.2015.00084.
43. Wang JY, Haider I, Jamil M et al (2019) The apocarotenoid metabolitezaxinone regulates growth and strigolactone biosynthesis in rice. Nat 10:810. https://doi.org/10.1038/s41467-019-08461-1
44. Wang L, Xu Q, Yu H et al (2020) Strigolactone and karrikin signaling pathways elicit ubiquitination and proteolysis of smxl2 to regulate hypocotyl elongation in Arabidopsis. Plant Cell 32:2251–

https://doi.org/10.1105/tpc.20.00140

45. Wang Y, Li J (2008) Molecular basis of plant architecture. Annu Rev Plant Biol 59:253– https://doi.org/10.1146/annurev.arplant.59.032607.092902
46. Wang Y, Shang L, Yu H, et al (2020) A Strigolactone Biosynthesis Gene Contributed to the Green Revolution in Rice. Mol Plant 13:923-932. https://doi.org/10.1016/j.molp.2020.03.009
47. Waterhouse A, Bertoni M, Bienert S et al (2018) SWISS-MODEL: homology modelling of protein structures and complexes. Nucleic Acids Res 46:296– https://doi.org/10.1093/nar/gky427
48. Waters MT, Nelson DC, Scaffidi A et al (2012) Specialisation within the DWARF14 protein family confers distinct responses to karrikins and strigolactones in Arabidopsis. Development 139:1285– https://doi.org/10.1242/dev.074567
49. Wen C, Xi L, Gao B et al (2015) Roles of DgD14 in regulation of shoot branching in chrysanthemum Dendranthema grandiflorum 'Jinba'. Plant Physiol Biochem 96:241– https://doi.org/10.1016/j.plaphy.2015.07.030
50. Xia Y, Huang G, Zhu Y (2019) Sustainable plant disease control: biotic information flow and behavior manipulation. Sci China Life Sci 62:1710-1713. https://doi.org/10.1007/s11427-019-1599-y
51. Xiao GH, Wang K, Huang G et al (2016) Genome-scale analysis of the cotton KCS gene family revealed a binary mode of action for gibberellin a regulated fiber growth. J Integr Plant Biol 58:577– https://doi.org/10.1111/jipb.12429
52. Xie Y, Liu Y, Ma M, et al (2020) Arabidopsis FHY3 and FAR1 integrate light and strigolactone signaling to regulate branching. Nat Commun 11:1955. https://doi.org/10.1038/s41467-020-15893-7
53. Yao R, Ming Z, Yan L et al (2016) DWARF14 is a non-canonical hormone receptor for strigolactone. Nature 536:469– https://doi.org/10.1038/nature19073
54. Yao R, Wang L, Li Y, et al (2018) Rice DWARF14 acts as an unconventional hormone receptor for strigolactone. J Exp Bot 69:2355– https://doi.org/10.1093/jxb/ery014
55. Yoshimura M, Sato A, Kuwata K et al (2018) Discovery of shoot branching regulator targeting strigolactone receptor DWARF14. ACS central science 4:230–234. https://doi.org/10.1021/acscentsci.7b00554
56. Zhang T, Hu Y, Jiang W et al (2015) Sequencing of allotetraploid cotton *Gossypium hirsutum* acc. TM-1 provides a resource for fiber improvement. Nat Biotechnol 33:531–537. https://doi.org/10.1038/nbt.3207
57. Zheng K, Wang X, Weighill DAet al (2016) Characterization of DWARF14 Genes in Populus. Sci Rep 6: https://doi.org/10.1038/srep21593

Figures

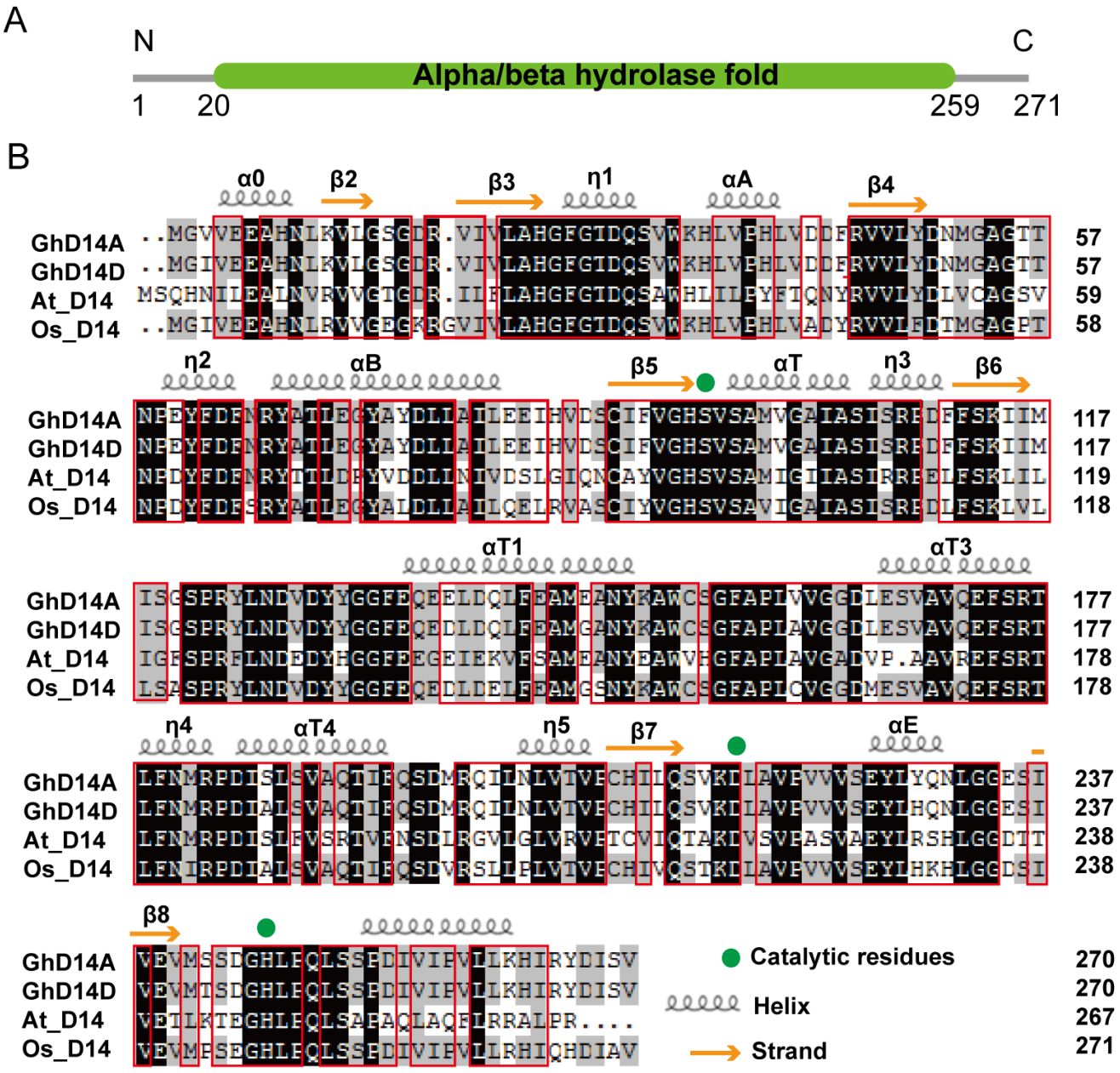

Figure 1

Multiple protein sequence alignment and structure diagram of D14 proteins. (A). D14 protein structure diagram. N indicates N-terminus; C indicates C-terminus. The green box indicates the alpha/beta hydrolase fold domain. The numbers below the protein represent the protein length and specific location of the domain. (B). Multiple protein sequence alignment of D14 proteins from cotton, Arabidopsis and rice. Secondary structure elements are displayed on top of the sequences. Identical and conserved residues are highlighted black and gray, respectively. The catalytic residues, helixes and strands are indicated by green dots, curved lines and orange arrows, respectively. Numbers on the right indicate the sequence length.

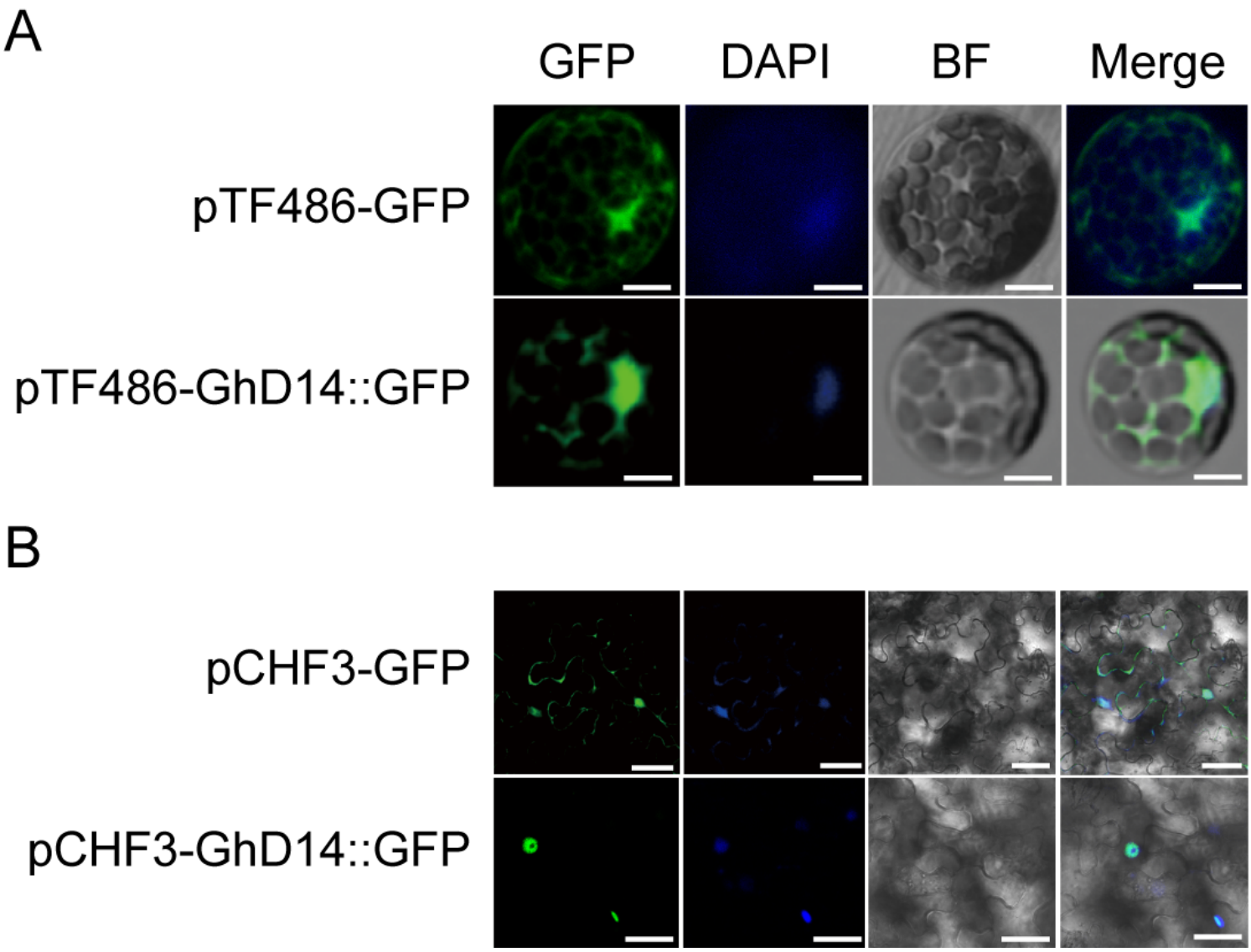

Figure 2

Subcellular localization of GhD14D protein. (A). Subcellular localization of GhD14D protein in Arabidopsis protoplasts. (B). Subcellular localization of GhD14D protein in tobacco epidermal cell. Pictures from left to right are GFP fluorescence, DAPI fluorescence, bright field (BF) and BF merged with DAPI and GFP fluorescence. Scale bars = 10 μm (A) and 50 μm (B).

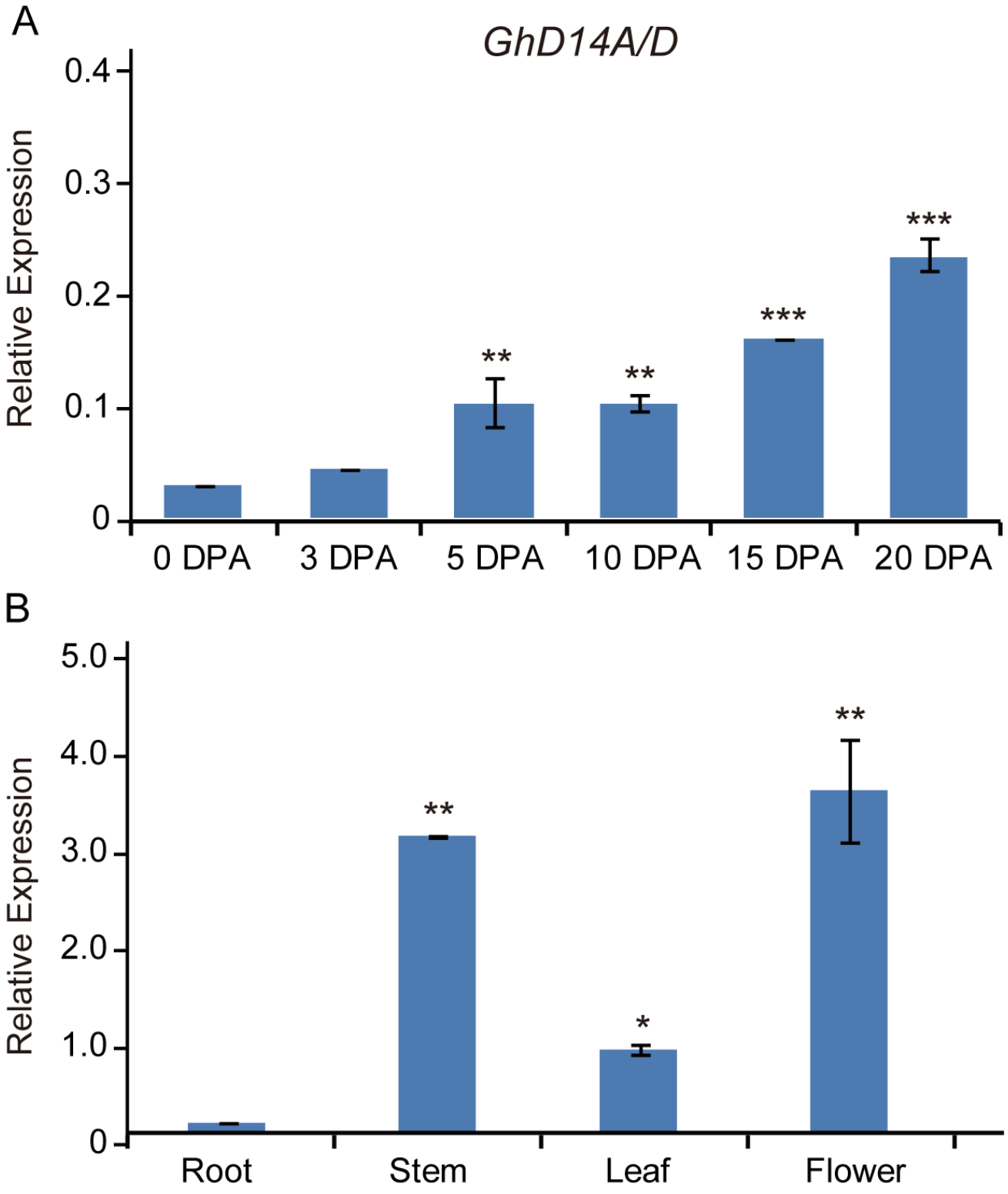

Figure 3

Expression analysis of GhD14A/D gene in different fiber development stages and tissues. The expression levels of GhD14A/D in fibers from 0 to 20 days post-anthesis (DPA) (A) and in different tissues (B). Statistical significance was determined using one-way ANOVA using 0 DPA samples (A) and root as the control (B), respectively. (* P<0.05; ** P<0.01; *** P<0.001).

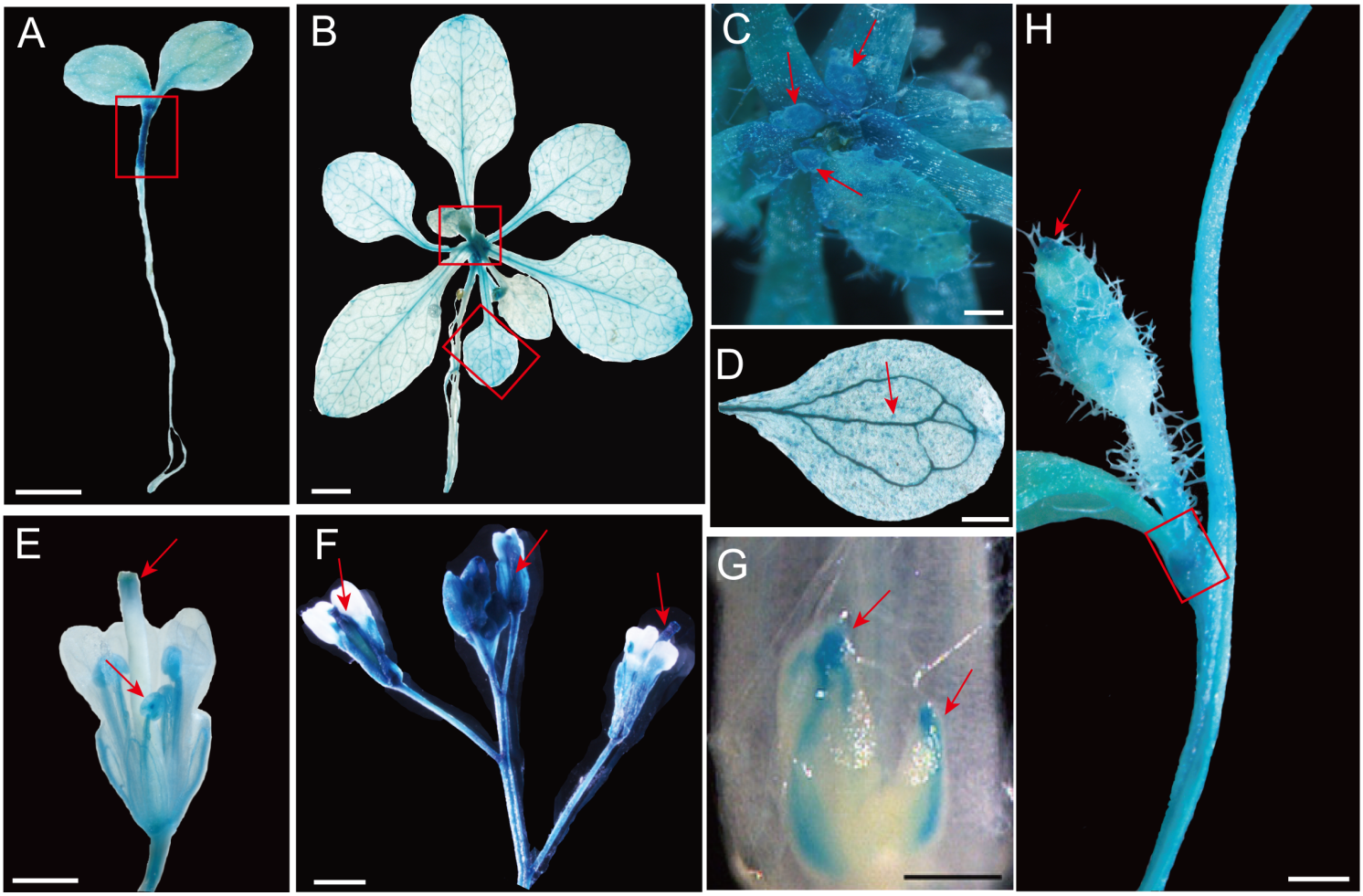

Figure 4

GUS staining assay of GhD14D gene promoter. The GUS staining result of 5-day-old transgenic seedings (A), 15-day-old transgenic plant (B), leaf primordium (C), cotyledon (D), flower (E), inflorescence (F), axillary bud (G) and stem (H). Scale bars = 0.2 mm in (A), 0.5 mm in (B), 1 mm in (C), 1 mm in (D), 0.5 mm in (E), 2 mm in (F), 1 mm in (G), and 2 mm in (H). The red rectangles and arrows indicate GUS staining locations.

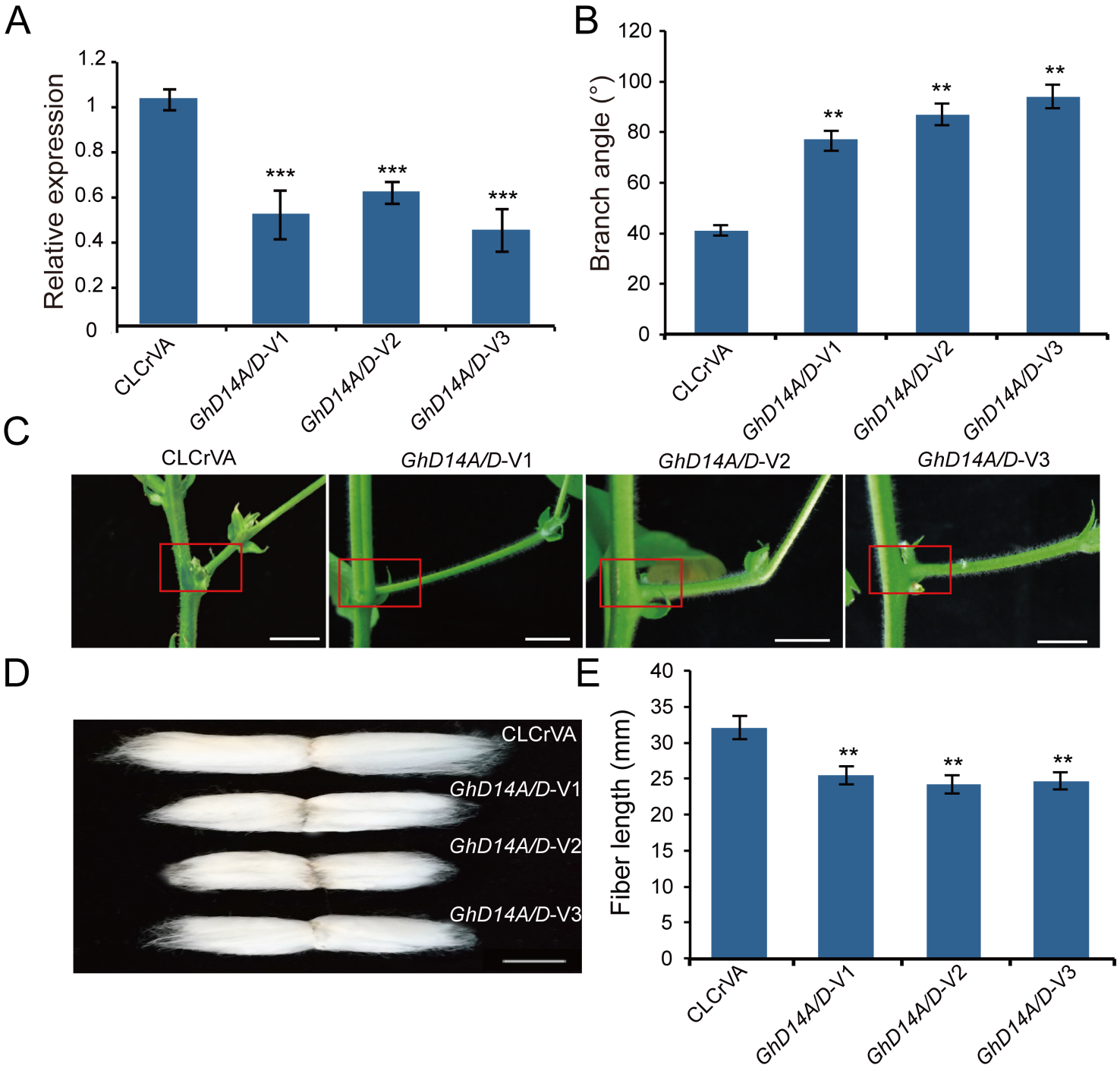

Figure 5

Silencing GhD14A/D modified plant architecture and reduced fiber length. (A). Relative expression levels of GhD14A/D in 25 DPA fibers from negative control (CLCrVA) and GhD14A/D-silenced cotton plants. (B). Average branch angles of negative control (CLCrVA) and GhD14A/D-silenced cotton plants. °, the degree of branch angle. (C). Branch phenotypes of negative control (CLCrVA) and GhD14A/D-silenced cotton plants. Red rectangles show the branch angles. Scale bars = 1 cm. (D). Representative seeds with attached fibers from negative control (CLCrVA) and GhD14A/D-silenced cotton plants. Scale bars = 1 cm. (E). Fiber length of negative control (CLCrVA) and GhD14A/D-silenced cotton plants. negative control (CLCrVA) and GhD14A/D-V1, GhD14A/D-V2, GhD14A/D-V3 represent cotton seedlings infiltrated with

pCLCrVA empty vector and pCLCrVA-GhD14A/D vector, respectively. Error bars represent the mean ± SE. Statistical significance was determined using one-way ANOVA. (** P<0.01; *** P<0.001).

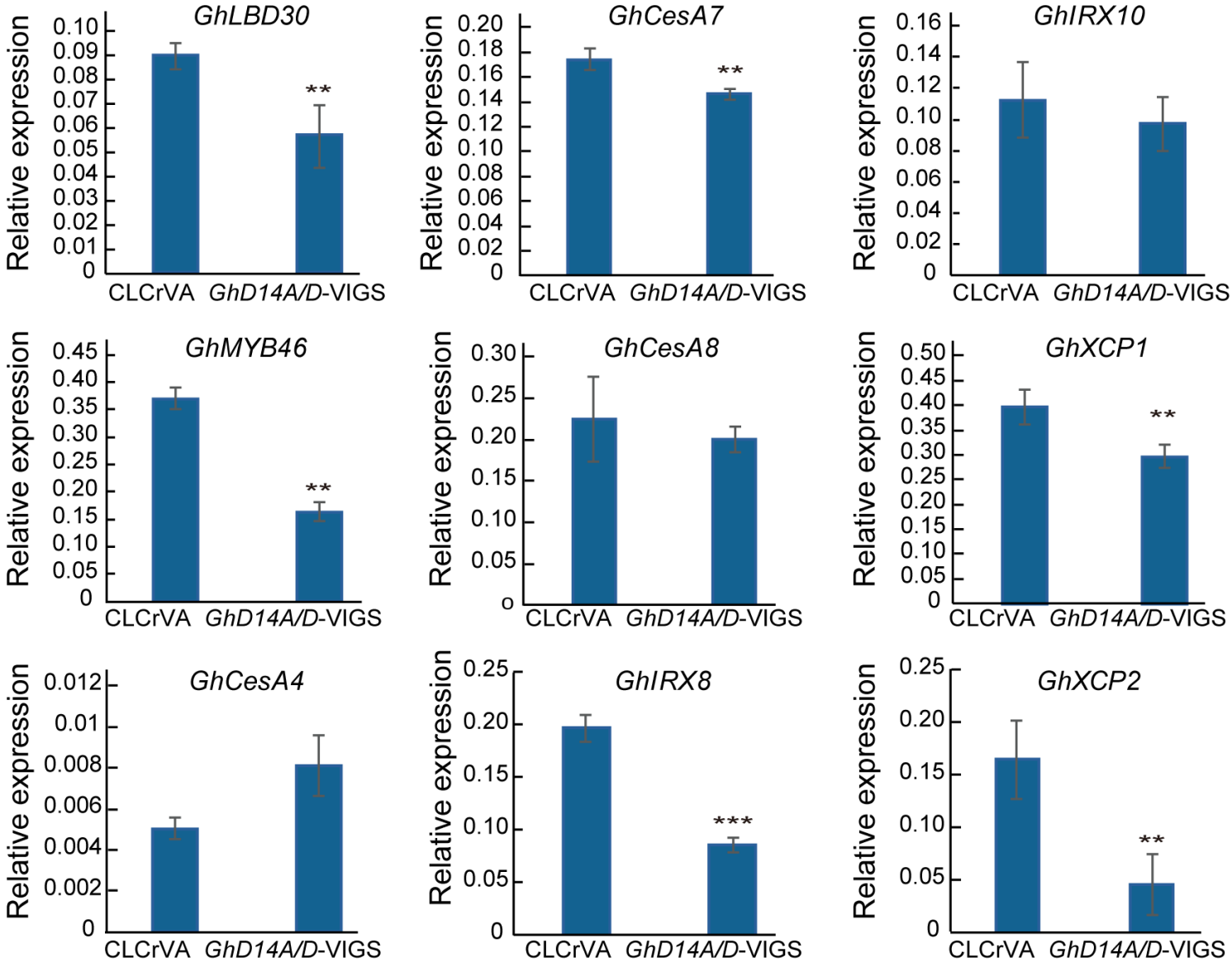

Figure 6

qRT-PCR analysis of secondary wall-associated formation genes. Relative gene expression of nine secondary cell wall biosynthesis genes in 20 DPA fibers of GhD14A/D-VIGS plants and negative control (CLCrVA) were calculated using GhUBQ7 as the internal reference gene. Error bars represent ± SE of triplicate experiments. Asterisks indicate statistically significant differences, as determined using one-way ANOVA (*P <0.05; **P <0.01).

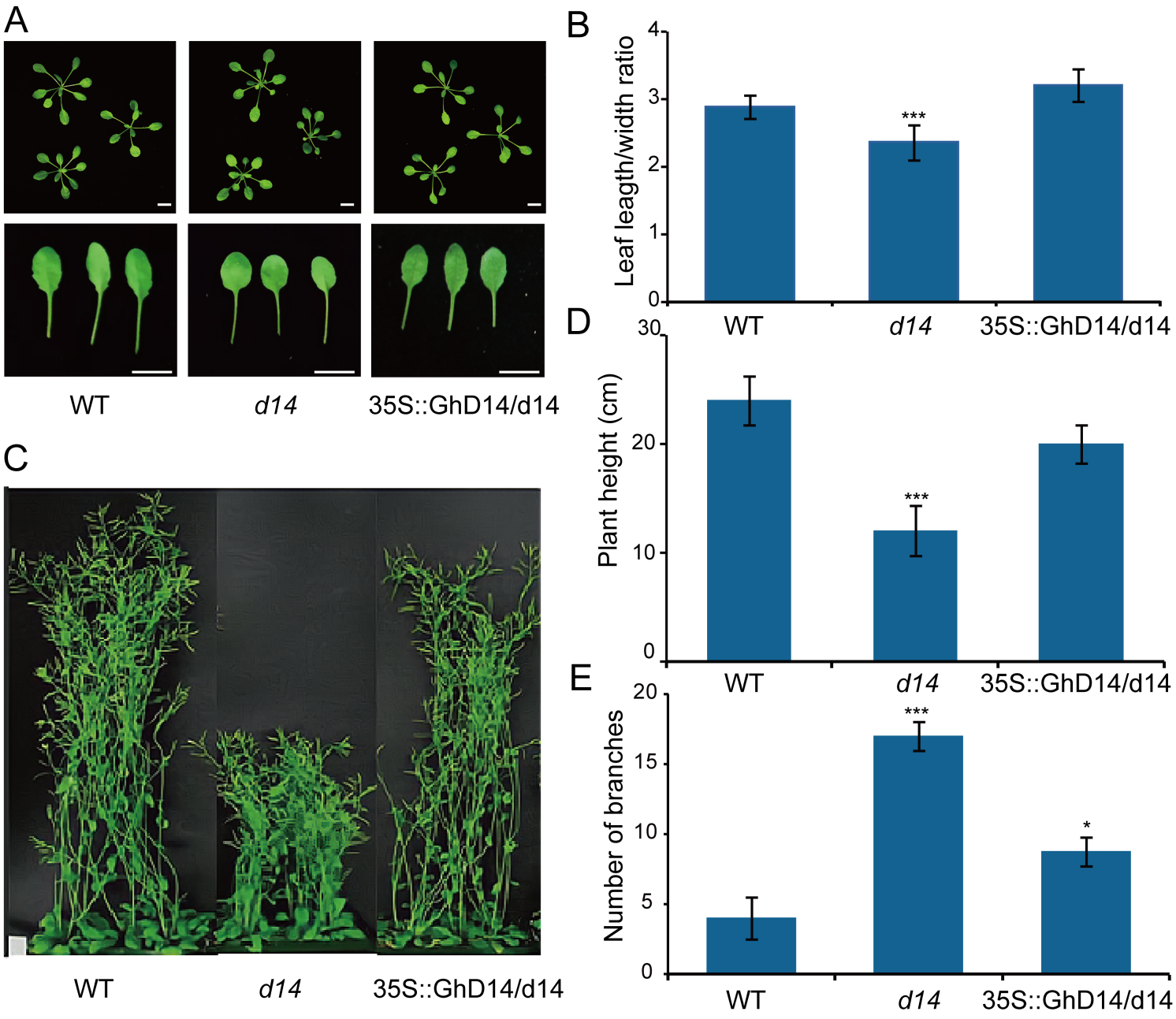

Figure 7

GhD14D recovered the d14 mutant phenotype in Arabidopsis. The rosette leaves (A) and plant height (C) phenotypes of WT, d14 mutant and GhD14D complementation line in d14 mutant background. Scale bars = 1 cm. Average length-width ratio (B), plant height (D) and average number of branches (E) of WT, d14 mutant and GhD14D complementation lines in the d14 mutant background. WT, wild type. Statistical analysis was performed with three biological replicates, and the error bars represent the mean ± SE. Statistical significance was determined using one-way ANOVA. (* P<0.05; *** P<0.001).

Supplementary Files

This is a list of supplementary files associated with this preprint. Click to download.

- Supplementalfiles.docx